Available online at www.sciencedirect.com
SCIENCE DIRECT
Talanta 69 (2006) 691–699
Talanta
www.elsevier.com/locate/talanta

Enzymatic rotating biosensor for ciprofloxacin determination

Angel A.J. Torriero, Juan J.J. Ruiz-Díaz, Eloy Salinas, Eduardo J. Marchevsky, María I. Sanz, Julio Raba *

Department of Chemistry, National University of San Luis, Chacabuco y Pedernera, 5700 San Luis, Argentina

Received 31 August 2005; received in revised form 31 October 2005; accepted 2 November 2005
Available online 15 December 2005

Abstract

The high sensitivity that can be attained using an enzymatic system and mediated by catechol has been verified by on-line interfacing of a rotating biosensor and continuous flow/stopped-flow/continuous-flow processing. Horseradish peroxidase, HRP [EC 1.11.1.7], immobilized on a rotating disk, in the presence of hydrogen peroxide, catalyzed the oxidation of catechol, whose back electrochemical reduction was detected on a glassy carbon electrode surface at −200 mV. Thus, when ciprofloxacin (CF) was added to the solution, this piperazine-containing compound participate in Michael addition reactions with catechol to form the corresponding piperazine–quinone derivatives, decreasing the peak current obtained, in proportion with the increase of its concentration. The highest response for CF was obtained around pH 7. This method could be used to determine CF concentration in the range of 0.02–65 μM ($r = 0.999$). The determination of CF concentration was possible with a detection limit of 0.4 nM, in the processing of as many as 25 samples per hour. Application of this analysis to different pharmaceutical samples containing CF supports the utility of the HRP-rotating biosensor.

Keywords: Ciprofloxacin; Glassy carbon; Biosensor; Peroxidase; Catechol; FIA

1. Introduction

Ciprofloxacin (CF) [1-cyclopropyl-6-fluoro-1,4-dihydro-4-oxo-7-(piperazinyl)quinolone-3-carboxylic acid] (Scheme 1), belongs to the quinolones, which are synthetic antibiotics, chemically related to nalidixic acid. These drugs form a group of antimicrobial agents with different chemical structures and spectra of activity.

Almost all of the recent clinically useful quinolones bear a fluorine atom in the C-6 position and thus, these antibacterial agents are called fluoroquinolones. Ciprofloxacin (belonging to the second-generation fluoroquinolone) is the most potent fluoroquinolone against Gram-positive and Gram-negative bacteria through inhibition of their NAD gyrase, a critical enzyme to bacterial chromosome replication [1,2]. It is used in a wide range of gastrointestinal, urinary, and respiratory tract infections; ocular and skin infections as well as in patients with intra-abdominal infections in combination with antianaerobic agents [3,4]. Recently, CF significance as effective drug in *Bacillus anthracis* infection treatment essentially increased, because of bacteriological (anthrax) terrorists' attack threats.

Therefore it is necessary to arrange sensitive and fast methods for determination of this antibacterial agent. Numerous methods have been reported for the determination of ciprofloxacin using techniques such as spectrophotometry [5–9], fluorimetry [8,10], high performance liquid chromatography with UV or fluorescence detection [11], capillary electrophoresis [12–15], and immunoassay [16]. Automatic methods based on flow injection analysis (FIA) have also been proposed using both spectrophotometric [17,18] and chemiluminescent [19] detection.

To the best of our knowledge, no study involving an enzymatic biosensor behavior for CF has been reported. Thus, in this paper, we present and discuss for the first time the electrochemical and enzymatic reaction for CF determination, which results in a single, fast and inexpensive analytical method, as well as a very sensitive devise based on HRP-rotating biosensor systems. The measuring principle of this biosensor is shown in Scheme 2. Horseradish peroxidase (HRP) in the presence of H_2O_2, catalyses the oxidation of catechol (Q) [20] whose electrochemical reduction back

* Corresponding author. Fax: +54 2652 43 0224.
E-mail address: jraba@unsl.edu.ar (J. Raba).

0039-9140/$ – see front matter © 2005 Elsevier B.V. All rights reserved.
doi:10.1016/j.talanta.2005.11.005

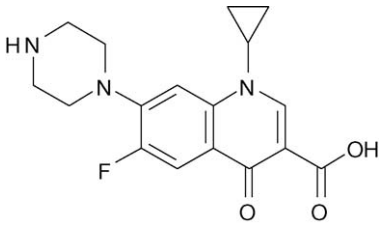

Scheme 1. Chemical structure of ciprofloxacin.

has a peak potential of 70 mV (see below). However, when piperazine-containing compound is added to the solution, it readily reacts with quinone derivative (P), through the Michael addition, decreasing the peak current obtained in proportion with the increase in concentration of the compound containing piperazine.

The initial reaction in the sequence (Q ⇆ P) is well established [21–23] by NMR, pulse radiolysis [21], and a number of electrochemical techniques [22,23] used to probe the mechanism. A substantial body of research has also been compiled which documents the possible physiological consequences of such reactions [24,25] The potential use of the second step (1) as a method of detecting CF is explored in this paper.

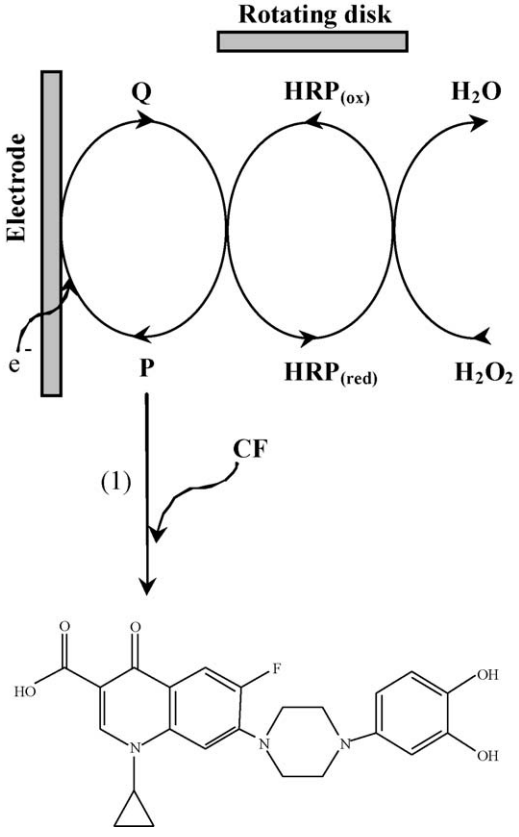

Scheme 2. Schematic representations of the reduction wave of the enzymatic process between catechol (Q), *o*-benzoquinone (P), hydrogen peroxide (H_2O_2), ciprofloxacin (CF) and Horseradish peroxidase (HRP).

2. Experimental

2.1. Reagents and solutions

All reagents used were of analytical reagent grade. The enzyme horseradish peroxidase, HRP [EC 1.11.1.7] Grade II, was purchased from Sigma Chemical Co., St. Louis. The concentration of HRP was determined spectrophotometrically using the Soret extinction coefficient of 102 $mM^{-1}\,cm^{-1}$ at 403 nm (181 IU mg^{-1}). Glutaraldehyde (25% aqueous solution) and hydrogen peroxide were purchased from Merck, Darmstadt. 3-Aminopropyl-modified controlled-pore glass with 1400 Å mean pore diameter and 24 $m^2\,mg^{-1}$ surface area, was purchased from Electro-Nucleonics (Fairfield, NJ) and contained 48.2 $\mu mol\,g^{-1}$ of amino groups. Catechol (0.1 M) was purchased from Sigma Chemical Co., St. Louis and generally used within 1 h. Ciprofloxacin stock standard solution (0.1 mg ml^{-1}) was prepared with exact measurements of ciprofloxacin hydrochloride (generously supplied by Northia laboratory, Argentina) dissolved in 0.02 N NaOH. This solution was stable for at least 1 week if stored away from light, at 4 °C. Working solutions were prepared by appropriate dilutions with a 0.10 M phosphate buffer (pH 7.00). All other reagents employed were of analytical grade and were used without further purification. All solutions were prepared with ultra-high-quality water obtained from a Barnstead Easy pure RF compact ultra pure water system, and the samples were diluted to the desired concentrations using a 10 ml Metrohm E 485 burette.

2.2. Flow-through sensor/detector unit

The main body of the cell was made of Plexiglas. Fig. 1 illustrates the design of the flow-through chamber containing the rotating enzyme biosensor and the detector system. Glassy carbon electrode (GCE) is found on the top of the rotating biosensor.

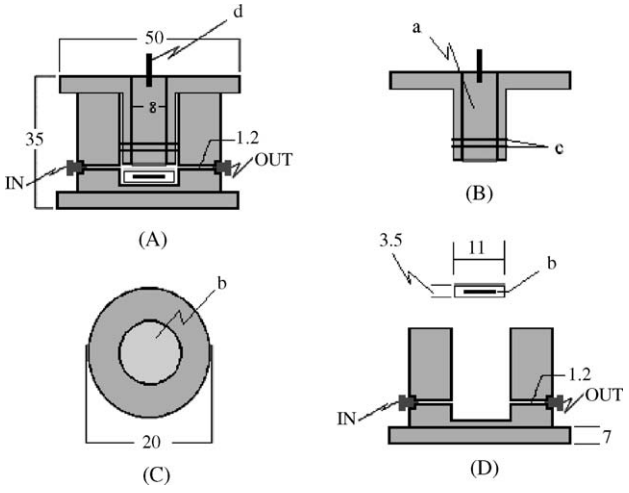

Fig. 1. Schematic representation of components in the biosensor flow cell. A, assembled sensor; B, upper cell body; C, top view of lower cell body; b, rotating biosensor (with immobilized HRP); D, lower cell body; a, glassy carbon electrode; b, rotating biosensor; c, O-ring; d, electrical connection. All measurements are given in millimeters.

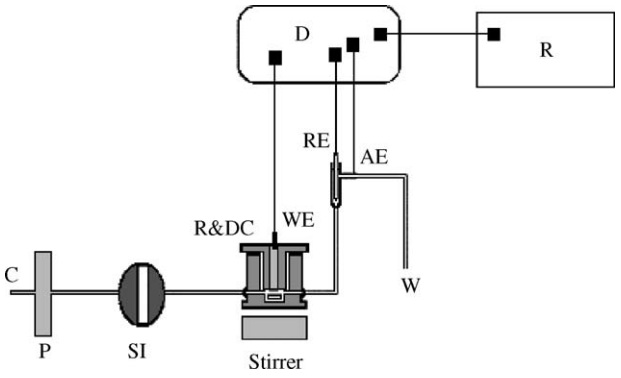

Fig. 2. Block diagram of the continuous-flow system and detection arrangement. P, pump (Gilson Minipuls 3 peristaltic pump, Gilson Electronics Inc., Middleton, WI); C, carrier buffer line; SI, sample injection; W, waste line; R&DC, sensor and detector cell; WE, glassy carbon electrode; RE, reference electrode (Ag/AgCl, 3.0 M NaCl); AE, auxiliary electrode (platinum); D, Potentiostat/Detection unit (CV27, Bioanalytical Systems, West Lafayette, IN); R, Recorder (Varian, Model 9176, Varian Techtron, Springvale, Australia).

The rotating biosensor is a disk of Teflon in which a miniature magnetic stirring bar (a Teflon-coated Micro Stir bar from Marksson Science Inc., Phoenix, AZ) has been embedded. Typically, a sensor disk carries 1.4 mg of controlled-pore glass on its surface. Rotation of the lower sensor was initiated by a laboratory magnetic stirrer (Metrohm E649 from Metrohm AG Herisau, Switzerland) and controlled with a variable transformer with an output between 0 and 250 V, and maximum amperage of 7.5 A (Waritrans, Argentina.). Amperometric detection was performed using a BAS LC-4C potentiostat and BAS 100 B/W (electrochemical analyzer Bioanalytical System, West Lafayette IN) was used to voltammetric determinations. The potential applied to the GCE for the functional group detection was −200 mV versus Ag/AgCl, 3.0 M NaCl reference electrode BAS RE-6, and a Pt wire counter electrode. At this potential, a catalytic current was well established.

A pump (Gilson Minipuls 3 peristaltic pump, Gilson Electronics Inc., Middleton, WI) was used for pumping, sample introduction, and stopping the flow. Fig. 2 illustrates schematically the components of the single-line continuous-flow setup. The pump tubing was Tygon (Fisher AccuRated, 1.0 mm i.d., Fisher Scientific Co., Pittsburgh, PA) and the remaining tubing used was Teflon, 1.00 mm i.d. from Cole-Parmer (Chicago, IL).

All pH measurements were made with an Orion Expandable Ion Analyzer (Orion Research Inc., Cambridge, MA), Model EA 940, which was equipped with a glass combination electrode (Orion Research Inc., Cambridge, MA). This pH-meter was calibrated with two buffers: biphthalate buffer, prepared by dissolving 2.53 g of potassium biphthalate in 250.0 ml of deionized water for pH 4.0 and tetraborate buffer, prepared by dissolving 0.95 g of sodium tetraborate in 250.0 ml of deionized water for pH 9.0.

2.3. Horseradish peroxidase immobilization

The rotating disk biosensor (bottom part) was prepared by immobilizing HRP on 3-aminopropyl-modified controlled-pore glass (APCPG). The APCPG, smoothly spread on one side of a double-coated tape affixed to the disk surface, was allowed to react with an aqueous solution of 5% (w/w) glutaraldehyde at pH 10.00 (0.20 M carbonate) for 2 h at room temperature. After washed with purified water and a 0.10 M phosphate buffer of pH 7.00, the enzyme (10.0 mg of enzyme preparation in 0.50 ml of 0.10 M phosphate buffer, pH 7.00) was coupled with residual aldehyde groups in phosphate buffer (0.10 M, pH 7.00), overnight, at 4 °C. The immobilized enzyme preparation was then washed with phosphate buffer (pH 7.00) and stored in the same buffer at 4 °C between uses. The immobilized HRP preparations were perfectly stable throughout at least 1 month of daily use.

2.4. Preparation of pharmaceuticals

Ten tablets were powdered and the amount corresponding to 100 mg of CF was weighed in a 250 ml volumetric flask, and 20 ml of 0.02 N NaOH solution was added. The flask was sonicated for 2 min and filled with 0.1 M phosphate buffer, pH 7.0. A small amount of non-dissolving excipients settled at the bottom of the flask. A 1 ml of the clear supernadant was transferred to a 100 ml volumetric flask and diluted to mark with 0.1 M phosphate buffer, pH 7.0. This was injected into the sample loop by means of a peristaltic pump.

In the injectable preparations, the entire content was put directly into a 250 ml volumetric flask and the procedure described above was followed.

In the ophthalmic solution a 1 ml volume of the ophthalmic solution 3 mg ml^{-1} (or 0.3% labeled concentration) in ciprofloxacin base, was quantitatively transferred to a 100 ml volumetric flask, 10 ml of 0.02 N NaOH solution was added and the solution was diluted to volume with 0.1 M phosphate buffer, pH 7.0. The resulting solution, having a labeled concentration of 30 $\mu g\ ml^{-1}$ in ciprofloxacin base was diluted with 0.1 M phosphate buffer, pH 7.0 by a factor of 10.

2.5. Preparation of synthetic tablet samples

Synthetic tablet samples were prepared in 100 ml calibrated flasks by spiking a placebo (mixture of tablet excipients) with accurately calculated amount of CF. Hereafter, the procedure described for the preparation of pharmaceuticals was followed.

2.6. Dosage forms of ciprofloxacin

(A) Ciriax tablets (Roemmers lab.): ciprofloxacin hydrochloride 500 mg; (B) Septicide tablets (Bago lab.): ciprofloxacin hydrochloride 500 mg; (C) Ciprotenk tablets (Biotenk Lab.): ciprofloxacin hydrochloride 500 mg; (D) Cipro tablets (Bayer Lab.): ciprofloxacin hydrochloride 500 mg; (E) Ciprofloxacin Northia tablets (Northia Lab.): ciprofloxacin hydrochloride 500 mg; (F) Ciprofloxacin Northia injectable (Northia Lab.): ciprofloxacin 200 mg; (G) Cipro otico colirium (Alcon Lab.): ciprofloxacin 3 mg ml^{-1}.

3. Results and discussion

3.1. Broad features of the amperometric detection of HRP in the presence of peroxide

Reactions catalyzed by enzymes have long been used for analytical purposes, determining different analytes such as substrates, inhibitors, and also enzymes. Biosensors, which combine the selectivity of enzymes with the high sensitivity of electrochemical measurements, have proved to be an excellent tool for analytical chemistry [26].

The mechanisms of HRP catalyzed reactions can be represented as follows (Scheme 3) [27]:

In the primary catalytic cycle of HRP, the kinetics of the reaction of E with H_2O_2 to yield E_1 has been investigated extensively [28,29]. Although evidence has previously been gathered that the kinetics follows a Michaelis–Menten behavior [30], it is only recently that its characteristics have been unambiguously determined [31], leading to $K_{1,M} = (k_{1,-1} + k_{1,2})/k_{1,1}$ (128 μM) and to a confirmation of the k_1 value (i.e. $k_1 = k_{1,1}k_{1,2}/(k_{1,-1} + k_{1,2}) = 1.7 \times 10^7\ M^{-1}\ s^{-1}$). The reduction of E_1 and E_2 by several electron donors has been reported where they are, in most cases, both electron and proton donors. Scheme 3 also indicates the possibility of a Michaelis–Menten behavior for the reduction of E_1 and E_2 in view of the fact that such behavior has been reported for several co-substrates.

Regarding the Michaelis–Menten behavior observed for the E_2/E reaction, it should be emphasized that the reduction of E_2 is not a mere outersphere electron-transfer reaction but rather involves the exchange of one electron and two protons, and the cleavage of the iron–oxygen bond (Scheme 4). These reactions, or possibly other unknown mechanistic peculiarities, may be the cause of the observed kinetics that shows saturation behavior when the reactant concentration is increased. Therefore the reaction does not necessarily reflect a true Michaelis–Menten mechanism such as the one depicted in Scheme 3.

Inhibition by conversion of the initial enzyme by H_2O_2 into inactive oxyperoxidase, E_3, may occur even in the presence of the oxidized form of the co-substrate. H_2O_2 may indeed reduce E_1 into E_2, albeit slowly [28], thus opening a route to the conversion of E_2 into E_3. Two pathways for this inactivation have been previously identified. One is an irreversible set of reactions yielding a verdohemoprotein (also designated as P670) [32]. This irreversible inactivation pathway of HRP is insignificant under our current experimental conditions. The second pathway involves the formation of oxyperoxidase [33], usually designated as compound III or E_3. This compound, which does not normally participate in the peroxidase activity of HRP, has a structure similar to that of oxyhemoglobin [34] (Scheme 5). In the presence of H_2O_2 the formation of E_3 from the reaction of H_2O_2 with E_2 occurs at a constant rate, k_4, ranging from 16 to 40 $M^{-1}\ s^{-1}$, depending on pH and temperature [35]. E_3 is not necessarily a dead the catalytic cycle of HRP, it is indeed converted back to E by spontaneous decomposition, yielding superoxide ion.

This fact can be observed easily in experimental form when varying H_2O_2 concentration from 2.5×10^{-5} to 5.0×10^{-3} M, for 20 μM Q solutions and several concentrations of HRP, whilst maintaining a constant Q concentration (Fig. 3). At low H_2O_2 concentration (0.025 mM), a linear relation can only be seen when the enzymes concentrations are low, losing this linearity as the enzymatic concentration increases. This change occurs because the H_2O_2 concentration is insufficient to generate maximum catalytic activity. With 0.1 mM H_2O_2 concentration, a perfect linearity within the concentration range studied is obtained. With 0.5 mM H_2O_2 concentration, the linearity is lost to low concentrations. This is due to the fact that the HRP is inactivated in excess of H_2O_2. At higher H_2O_2 concentrations, such as 5 mM,

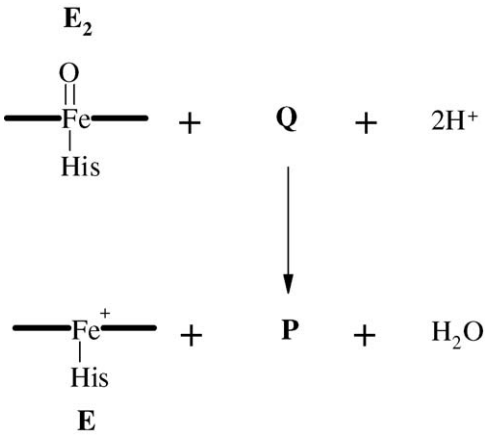

Scheme 4.

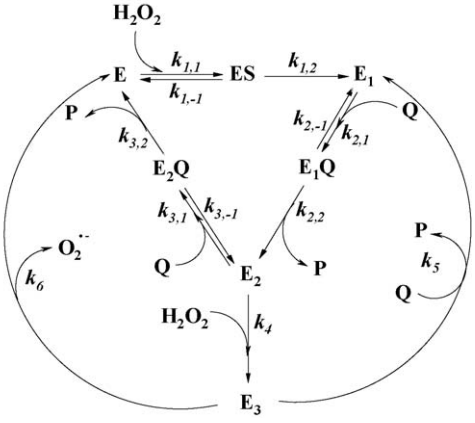

Scheme 3.

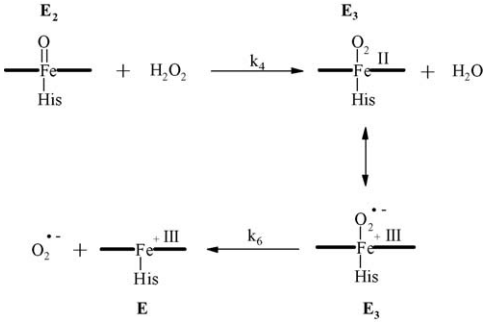

Scheme 5.

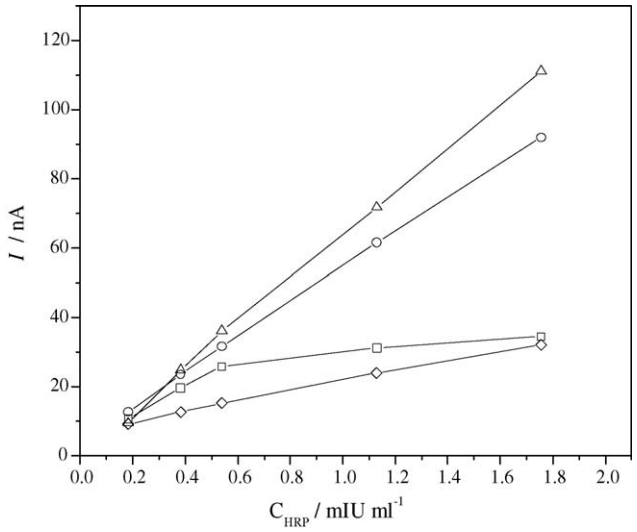

Fig. 3. Catalytic current as a function of the HRP concentration recorded at −200 mV vs. Ag/AgCl 3 M NaCl in a phosphate buffer (pH 7.00) containing 1.0 μM Q, and 0.025 (□), 0.1 (◯), 0.5 (△), and 5 (◇) mM H_2O_2.

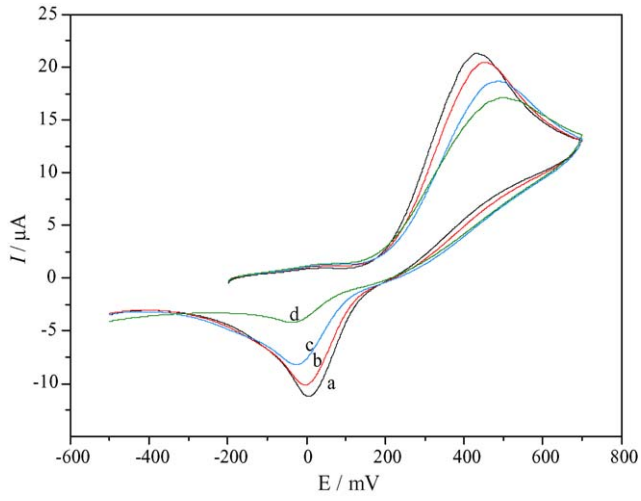

Fig. 5. Typical voltammograms of 1.0 mM Q at a glassy carbon electrode (3 mm diameter) in aqueous solution containing 0.1 M phosphate buffer (pH 7.00) at various CF concentrations, C_{CF}: (a) 0.0, (b) 0.18, (c) 0.34, and (d) 0.58 mM. Scan rate: 100 mV s^{-1}; T: 25 ± 1 °C.

inhibition by conversion of the initial enzyme by H_2O_2 into E_3 is observed throughout the entire HRP concentration range studied. In this case linearity is observed but the catalytic current obtained is less significant than in the optimal case.

3.2. Electrooxidation of catechol in the absence and presence of ciprofloxacin

Cyclic voltammetry of a 1 mM solution of catechol (Q) in an aqueous solution containing 0.10 M phosphate buffer pH 7.0 as a supporting electrolyte, shows one anodic (A_1) and a corresponding cathodic peak (C_1), both of which correspond to the transformation of Q to *o*-benzoquinone and vice versa within a quasi-reversible two-electron process (Fig. 4, curve a). A peak current ratio ($I_p^{C_1}/I_p^{A_1}$) of near unity, particularly during the repetitive recycling of potential, can be considered as a criterion for the stability of *o*-quinone produced at the surface of the electrode under the experimental conditions. In other words, all hydroxylation [36–39] or dimerization [40,41] reactions are too slow to be observed on the time scale of cyclic voltammetry. The oxidation of Q in the presence of CF as a nucleophile was also studied. Fig. 4, curve b, shows the cyclic voltammogram obtained for a 1 mM solution of Q in the presence of 0.58 mM CF. The voltammogram exhibits an anodic peak at 542 mV versus Ag/AgCl 3 M NaCl, and the cathodic counterpart of the anodic peak A_1 tends to disappear.

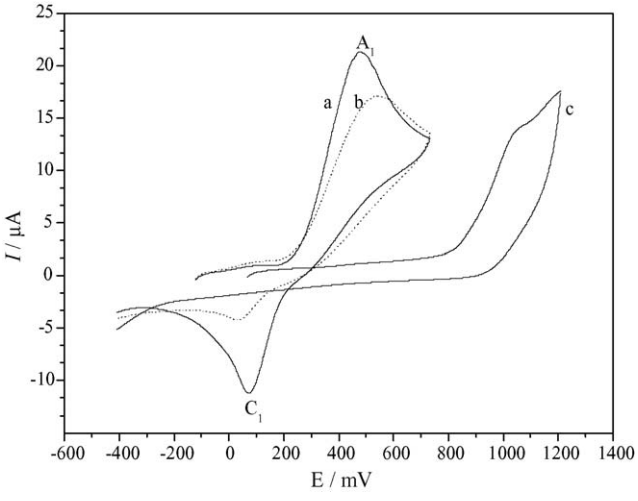

Fig. 4. Cyclic voltammograms of 1 mM Q: (a) in the absence, (b) in the presence of 0.58 mM CF, and (c) 0.44 mM CF in the absence of Q, at glassy carbon electrode (3 mm diameter) in aqueous solution containing 0.1 M phosphate buffer (pH 7.00). Scan rate: 100 mV s^{-1}; T: 25 ± 1 °C.

The influence of increasing CF concentration on the electrochemical behavior of Q was also investigated and subsequent responses are shown in Fig. 5. The height of the oxidation peak was found to decrease with increasing additions of CF, resulting in the loss of the corresponding reduction peak consistent with the EC type mechanism proposed in Scheme 2. The successive decrease in the height of the Q oxidation and reduction peaks can be maybe linked to the fact that the increasing concentration of CF serve to scavenge the oxidized form of Q such that on the forward and reverse sweep there is little available to participate in the electrochemical reaction.

Given that the direct oxidation of CF at the electrode does not occur within the potential window studied (Fig. 4, curve c), the decrease in the magnitude of the Q oxidation peak can be attributed solely to the Q–CF adduct formation.

The influence of pH on the peak potential (E_p) of the reaction was assessed through examining the electrode response to Q–CF obtained in solutions buffered between pH 4 and pH 8. The position of the redox couple was found to be dependent upon pH with a shift of 61 mV pH^{-1}, indicative of *n* electron *n* proton behavior with *n* likely to be two [42]. A quantitative evaluation of the Q change peak current (ΔI) response to increasing additions of CF, as a function of solution pH, is highlighted in Table 1. The ΔI reported hereafter is the difference between the reduction current (from addition of Q) and the current due to the addition

Table 1
Influence of pH on the magnitude of the oxidation signal for 1.00 mM Q in the presence of several CF concentrations

CF added (μM)	ΔI (μA) ± S.D.			
	pH 4.00	pH 5.00	pH 6.00	pH 7.00
0	0	0	0	0
20	3.13 ± 0.01	5.59 ± 0.01	8.50 ± 0.01	10.85 ± 0.01
40	5.27 ± 0.02	11.44 ± 0.02	16.73 ± 0.02	21.67 ± 0.02
60	8.01 ± 0.01	16.96 ± 0.02	24.99 ± 0.02	32.03 ± 0.03
80	9.73 ± 0.01	21.46 ± 0.03	32.79 ± 0.02	41.19 ± 0.02
100	11.82 ± 0.02	26.23 ± 0.02	39.42 ± 0.03	48.43 ± 0.03
120	13.88 ± 0.02	30.39 ± 0.03	44.56 ± 0.03	55.03 ± 0.04
140	15.58 ± 0.03	33.13 ± 0.03	48.37 ± 0.03	60.49 ± 0.03
160	17.30 ± 0.03	35.55 ± 0.03	51.48 ± 0.03	64.72 ± 0.04

of CF. The subsequent response was that decreased steadily as the acidity of the solution was increased. This can be attributed to the fact that as the pH of the solution was lowered, the piperazine functionality increasing protonated (CF, p$K_a \sim 8.24$) and hence the nucleophilic character of the piperazine moiety diminished. Increasing the pH clearly improves the response, but an operational limit is reached once neutral conditions prevail. Alkaline solution severely compromises the enzyme stability as well as the response; as the increased presence of nucleophilic hydroxyl ions compete with the less prevalent piperazine compound. Therefore, the pH value used was 7.00 in 0.1 M phosphate buffer in concordance with the steadier pH of the enzyme.

3.3. Effect of biosensor rotation and continuous-flow/stopped-flow operation

The implementation of continuous-flow/stopped-flow programming and the location of two facing independent biosensors (Fig. 2), permits: (a) utilization of relatively low enzyme loading conditions, (b) instantaneous operation under high initial rate conditions, (c) easy detection of accumulated products, and (d) reduction of the apparent Michaelis–Menten constant, K'_M. Therefore, a more complete reagent homogenization is achieved because the cell works as a mixing chamber by facilitating the arrival of substrate at the active sites and the release of products from the same sites. The net result is high values of current (see Table 2). The main advantages of this system are its simplicity and the ease with which it can be applied to the determination of CF at low levels.

Table 2
Values of K'_M (apparent Michaelis–Menten constant)

Rotation velocity (rpm)	K'_M (mM)[a]	Linear regression, standard deviation
170	23.53	±0.39
240	15.69	±0.26
420	8.91	±0.37
600	5.19	±0.19
840	2.54	±0.32
900	2.13	±0.17
[b]	280.03	±0.33

Determined as discussed in the text (temperature 20 ± 1 °C).
[a] Each value of K'_M based on triplicate of six different substrate concentrations.
[b] Estimated free enzyme in solution.

If the sensor in the cell is devoid of rotation, there is practically no response. If a rotation of 900 rpm is imposed on the sensor located at the bottom of the cell (with immobilized HRP), the signal is dramatically enlarged. As shown in traces d in Fig. 6, if the lower sensor is devoid of rotation the response is lower because diffusional limitations control the enzyme-catalyzed reaction. This trend indicates that, up to velocities of about 900 rpm, a decrease in the thickness of the stagnant layer improves mass transfer to and from the immobilized enzyme active sites. Beyond 900 rpm, the initial rate is constant and chemical kinetics control the overall process. As observed earlier [43], although the mass transfer is taking place under conditions similar to a thin-layer bounded diffusion with imposed turbulence, the dependence seems to agree with the response at a rotating disk electrode. Fig. 6 shows the effect of rotation under continuous- and stopped-flow conditions. Response to 1.0 mM Q under continuous flow is relatively small but comparatively larger if the sensor is rotated (compare traces b and c in Fig. 6). It produces a significant signal that increases almost linearly over time when the disk is rotated. Under stopped-flow conditions there is also a response, but smaller than with rotation. These responses indicate that the utilization of the biocatalytic action of the immobilized enzyme preparations is better under rotation of the sensor at the bottom of the cell.

The current developed at the detector should be directly proportional to the concentration of analyte in the bulk of the solution and should also increase with increasing rotation velocity. If the flow is stopped when the sample plug transported by continuous flow reaches the center of the sensor, detection takes place under conditions similar to those of batch detection [44].

3.4. Effect of cell volume and sample size

Depending on the volume of the cell in contact with the sensors, the overall process becomes controlled by diffusion (large volumes) or by the chemical kinetics of the enzyme-catalyzed reactions (small volumes). The cell volume was changed from 200 μl to 1 ml by removing the O-rings between the upper and lower half of the cell. The measured current, as expected, decreased linearly with an increase in cell volume. This was due to the dilution effect favored by rotation and the fact that

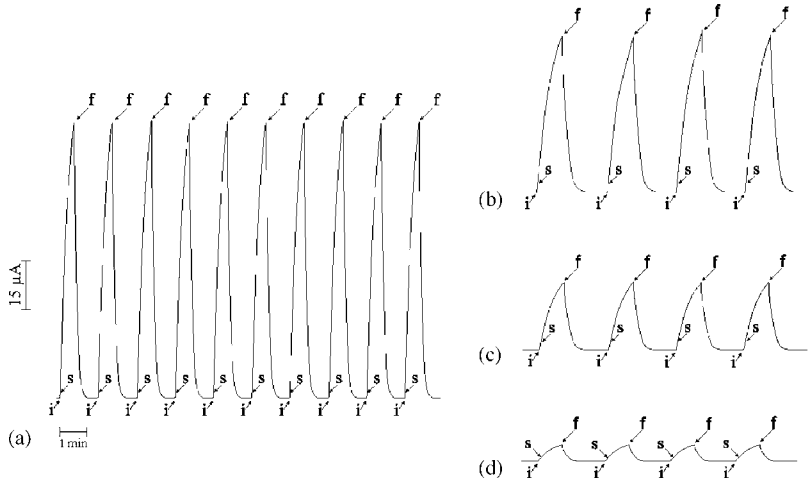

Fig. 6. Effect of sensor rotation under continuous and stopped-flow conditions. (a) Stopped-flow with rotation, (b) continuous-flow with rotation, (c) stopped-flow without rotation, and (d) continuous-flow without rotation. The solution containing 0.1 mM H_2O_2 and 1.0 mM Q in 0.1 M phosphate buffer, pH 7.00. Flow rate was 1.00 ml min^{-1} and cell volume was 200 μl. The flow was stopped for 60 s during measurement.

the measured current is directly proportional to bulk concentration. The smallest cell volume of 200 μl was adopted for further studies.

The measured current increased linearly with sample size, up to 200 μl, in a cell with a volume of 200 μl. For convenience a sample size of 200 μl was used. Sensitivity is almost tripled in the range between 50 and 200 μl (Table 3).

3.5. CF measurement with HRP-rotating biosensor

The performance of the HRP-rotating biosensor for the measurement of CF concentrations was characterized. For CF measurement, the following procedure was used: (a) a baseline current was established with the buffer solution; (b) a solution containing 1 mM Q and 0.1 mM H_2O_2 were injected into the rotating biosensor; (c) the flow was detained and the disk was rotated to 900 rpm, thus, a large reduction current was observed due to the quinone derivative and after 1 min the flow was started again; (d) a solution containing 1 mM Q, 0.1 mM H_2O_2, and several CF concentrations was injected into the rotating biosensor; (e) the flow was detained and the disk was rotated to 900 rpm, and the reduction current was measured. The addition of CF resulted in a current decrease. After 1 min the flow was started again. A CF calibration plot was obtained by plotting ΔI versus CF concentration.

A linear relation [Eq. (1)] was observed between the ΔI and the CF concentration in the range of 0.02–65 μM (rotation 900 rpm) using this method.

$$\Delta I\,(\mu A) = 0.21 + 0.52[C_{CF}] \quad (1)$$

The correlation coefficient for this type of plot was typically 0.999. Detection limit (DL) is the minimal difference of concentration that can be distinguished from the signal of the pure Q solution. The DL was calculated as the amount of CF required to

Table 3
Effect of sample size[a]

Sample size (μl)	I (μA)	Linear regression, standard deviation
50	5.82	±0.28
75	14.20	±0.17
100	23.80	±0.14
125	36.45	±0.29
150	51.39	±0.15
175	60.65	±0.21
200	64.60	±0.18
225	65.02	±0.33
250	64.57	±0.30
300	64.68	±0.27

Solution containing 0.1 mM H_2O_2 and 1.0 mM Q in 0.1 M phosphate buffer, pH 7.00. Flow rate, 1.00 ml min^{-1}.

[a] The current was measured under stopped-flow conditions. Each value of current is based on triplicate of six determinations.

Table 4
Precision and recovery rates for CF, obtained with HRP-rotating biosensor

Added mg	Found (mg) ± S.D.	Recovery (%)	VC (%)
5.00	5.02 ± 0.05	100.4	1.0
10.00	9.98 ± 0.09	99.8	0.9
15.00	15.04 ± 0.19	100.3	1.3
20.00	19.95 ± 0.28	99.7	1.4

Table 5
Specificity results of the HRP-rotating biosensor[a]

Sample number	Pure sample, 15.0 (μg ml^{-1})	Synthetic tablet sample (n = 5), X (μg ml^{-1})
1	15.15	15.10
2	14.77	14.80
3	15.12	15.12
4	14.89	14.85
5	15.21	15.20
6	14.80	14.85
X	14.99 ± 0.08	14.98 ± 0.07
S.D.	0.19	0.17
VC (%)	0.53	0.47

[a] X (μg ml^{-1}), mean ± S.E., standard error; S.D., standard deviation; VC, variation coefficient.

Table 6
Determination by the developed method of amount of CF contained in various CF formulations[a]

Sample number	Brand A (g/tablet)	Brand B (g/tablet)	Brand C (g/tablet)	Brand D (g/tablet)	Brand E (g/tablet)	Brand F (g/injectable)	Brand G (mg/ml)
1	0.498	0.515	0.509	0.488	0.490	0.201	2.85
2	0.474	0.512	0.484	0.481	0.532	0.202	3.37
3	0.506	0.509	0.516	0.519	0.489	0.204	2.94
4	0.510	0.479	0.515	0.527	0.485	0.199	2.99
5	0.488	0.491	0.480	0.512	0.494	0.198	3.17
6	0.512	0.485	0.495	0.486	0.519	0.199	3.39
7	0.489	0.522	0.507	0.515	0.508	0.201	2.80
8	0.492	0.493	0.519	0.482	0.514	0.198	2.91
X	0.496	0.501	0.503	0.501	0.504	0.200	3.05
S.D.	0.013	0.016	0.015	0.019	0.017	0.002	0.230

[a] For Brand name see dosage forms of ciprofloxacin.

yield a net peak that was equal to three times the S.D. of the pure Q signal. In this study, the minimal difference of concentration of CF was ca. 0.4 nM. Quantification limit (QL) was generally determined by the samples with known concentrations of analyte and by establishing the minimum level at which the analyte can by quantified with acceptable accuracy and precision [45]. The precision for CF was established by analyzing eight different standard solutions containing the lowest concentration on the calibration graph. The variation coefficient (VC) was 11% (it should be <20%).

Reproducibility assays were made using repetitive standards solutions ($n=5$) containing 1.0 mM Q, 0.1 mM H_2O_2, and 12 μM CF, and the percentage standard error was less than 3%.

Recovery studies were performed by adding a synthetic mixture prepared according to the manufacturer's batch formula (starch, lactose, magnesium stearate, hydroxypropylmethyl cellulose, cellulose micro-crystalline, and titanium oxide) to known amount of CF. The mean recovery was 100.05% (Table 4).

For the specificity test, a synthetic tablet of CF containing excipients (see recovery) was recorder at selected conditions. The response of the synthetic tablet was compared with the response of pure CF. It was found that assay results were not changed. Therefore, excipients commonly found in typical pharmaceutical preparations did not interfere with the quantization of CF present as an active principle. The results are showed in Table 5.

The stability of the biosensor was tested by nearly 3 h of continuous use in the FIA system. In this experiment, after every four samples, a standard solution containing 1.0 mM Q, 0.1 mM H_2O_2, and 12 μM CF was injected to test the electrode response. In the FIA system using an enzymatic sensor, there is practically no decay in the catalytic current after eight samples.

The developed method for the CF determination was applied to seven different commercial preparations (Table 6). There is no need for any extraction procedure before HRP-rotating biosensor analysis.

4. Conclusions

The usefulness of enzyme biosensor as a determiner of very low concentrations of CF was demonstrated. The biosensor developed in this work is the first one developed for CF determination. This type of detection (addition reaction on co-substrates) shows promise with regards to biological and pharmacological sensing. Also, this biosensor is able to operate as a fast, selective and sensitive detection unit when is incorporated into a FIA system. It provides a fast and cost effective solution to the realization of quantitative information at extremely low levels of CF concentrations.

Acknowledgements

The authors wish to thank the Universidad Nacional de San Luis and the Consejo Nacional de Investigaciones Científicas y Técnicas (CONICET) for their financial support. One of the authors (A.A.J.T.) acknowledges support in the form of a fellowship from the Consejo Nacional de Investigaciones Científicas y Técnicas (CONICET).

References

[1] Directors of the American Society of Hospital Pharmacists, Drug Information 88, Bethesda, MD, 1988, pp. 415–420.
[2] World Health Organization Meeting, Use of Quinolones in Food Animals and Potential Impact on Human Health, Geneva, Switzerland, 1998.
[3] R. Davis, A. Markham, J.A. Balfour, Drugs 51 (1996) 1019.
[4] J.S. Solomkin, H.H. Reinhart, E.P. Dellinger, Ann. Surg. 223 (1996) 303.
[5] M.I. Pascual-Reguera, G. Pérez Parra, A. Molina Díaz, J. Pharm. Biomed. Anal. 35 (2004) 689.
[6] B.S. Nagaralli, J. Seetharamappa, M.B. Melwanki, J. Pharm. Biomed. Anal. 29 (5) (2002) 859.
[7] S. Mostafa, M. El-Sadek, E.A. Alla, J. Pharm. Biomed. Anal. 27 (2002) 133.
[8] M. Rizk, F. Belal, F. Ibrahim, S. Ahmed, Z.A. Sheribah, J. AOAC Int. 84 (2) (2001) 368.
[9] The United States Pharmacopoeia, XXVI Revision, 2003.
[10] A. Navalón, O. Ballesteros, R. Blanc, J.L. Vílchez, Talanta 52 (2002) 845.
[11] G. Carlucci, J. Chromatogr. A 812 (1998) 343.
[12] M. Hernández, C. Aguilar, F. Borrull, M. Calull, J. Chromatogr. B Anal. Technol. Biomed. Life Sci. 772 (1) (2002) 163.
[13] C. Fierens, S. Hillaert, W. Van den Bossche, J. Pharm. Biomed. Anal. 22 (5) (2000) 763.
[14] Ph. Schmitt-Kopplin, J. Burhenne, D. Freitag, M. Spiteller, A. Kettrup, J. Chromatogr. A 837 (1–2) (1999) 253.

[15] D. Barrón, E. Jimenez-Lozano, J. Cano, J. Barbosa, J. Chromatogr. B 759 (2001) 73.
[16] G.G. Snitkoff, D.W. Grabe, R. Holt, G.R. Bailie, J. Immunoassay 19 (4) (1998) 227.
[17] S.M. Sultan, F.O. Suliman, Analyst 117 (9) (1992) 1523.
[18] F.O. Suliman, S.M. Sultan, Talanta 43 (4) (1996) 559.
[19] F.A. Aly, S.A. Al-Tamimi, A.A. Alwarthan, Talanta 53 (2001) 885.
[20] C. Ruan, Y. Li, Talanta 54 (2001) 1095.
[21] C.J. Cooksey, K. Jimbow, E.J. Land, P.A. Riley, Melanoma Res. 2 (1992) 283.
[22] M.J. Picklo, V. Amarnath, D.G. Graham, T.J. Montine, Free Radic. Biol. Med. 27 (1999) 271.
[23] H.T. Deng, G.J. Van Berkel, Electroanalysis 11 (1999) 857.
[24] X.M. Shen, B. Xia, M.Z. Wrona, G. Dryhurst, Chem. Res. Toxicol. 9 (1996) 1117.
[25] T.J. Montin, M.J. Picklo, V. Amarnath, W.O. Whetsell, D.G. Graham, Exp. Neurol. 148 (1997) 26.
[26] G.G. Guilbault, Marcel Dekker, New York, 1984, pp. 211–231.
[27] M. Dequaire, B. Limoges, J. Moiroux, J.M. Savéant, J. Am. Chem. Soc. 124 (2002) 240.
[28] J. Hernandez-Ruiz, M.B. Arnao, F. Garcia-Canovas, M. Acosta, Biochem. J. 354 (2001) 107.
[29] A. Asokan, J.S. De Ropp, S.L. Newmyer, P.R. Ortiz de Montellano, G.N. Mar, J. Am. Chem. Soc. 123 (2001) 4243.
[30] H.K. Baek, H.E. Van Wart, Biochemistry 28 (14) (1989) 5714.
[31] J.N. Rodriguez-Lopez, M.A. Gilabert, J. Tudela, R.N.F. Thorneley, F. Garcia Canovas, Biochemistry 39 (43) (2000) 13201.
[32] R. Nakajima, I. Yamazaki, J. Biol. Chem. 255 (1980) 2067.
[33] J.B. Wittenberg, R.W. Noble, B.A. Wittenberg, E. Antonini, M. Brunori, J. Wyman, J. Biol. Chem. 242 (1967) 626.
[34] D. Cai, M. Tien, Biochemistry 29 (8) (1990) 2085.
[35] R.W. Noble, Q.H. Gibson, J. Biol. Chem. 245 (1970) 2409.
[36] L. Papouchado, G. Petrie, R.N. Adams, J. Electroanal. Chem. 38 (1972) 389.
[37] L. Papouchado, G. Petrie, J.H. Sharp, R.N. Adams, J. Am. Chem. Soc. 90 (1968) 5620.
[38] T.E. Young, J.R. Griswold, M.H. Hulbert, I. Melanin, J. Org. Chem. 39 (1974) 1980.
[39] A. Brun, R. Rosset, J. Electroanal. Chem. 49 (1974) 287.
[40] D.L. Stom, S.N. Suslov, Biofizika 21 (1979) 40.
[41] M.D. Ryan, A. Yueh, C. Wen-Yu, J. Electrochem. Soc. 127 (1980) 1489.
[42] W.J. Albery, Electrode Kinetics, Clarendon Press, Oxford, 1975.
[43] P. Richter, B. López Ruiz, M. Sánchez-Cabezudo, H.A. Mottola, Anal. Chem. 68 (1996) 1701.
[44] R.A. Kamin, G. Wilson, Anal. Chem. 52 (1980) 1198.
[45] Third International Conference on Harmonization of Technical Requirement for Registration of Pharmaceuticals for Human Use, 1995, Japan.